Nuclear Medicine and Biology 72–73 (2019) 26–35

Contents lists available at ScienceDirect

Nuclear Medicine and Biology

journal homepage: www.elsevier.com/locate/nucmedbio

VMAT2 imaging agent, D6-[^{18}F]FP-(+)-DTBZ: Improved radiosynthesis, purification by solid-phase extraction and characterization

Ruiyue Zhao [a,b], Zhihao Zha [b,c], Xinyue Yao [a,b], Karl Ploessl [c], Seok Rye Choi [c], Futao Liu [a], Lin Zhu [a], Hank F. Kung [b,c,*]

[a] College of Chemistry, Beijing Normal University, Beijing 100875, PR China
[b] Department of Radiology, University of Pennsylvania, Philadelphia, PA 19104, USA
[c] Five Eleven Pharma Inc., Philadelphia, PA 19104, USA

ARTICLE INFO

Article history:
Received 3 April 2019
Received in revised form 6 June 2019
Accepted 6 July 2019
Available online xxxx

Keywords:
VMAT2
^{18}F
Deuterium
Tetrabenazine
SPE purification
Parkinson's disease

ABSTRACT

Objectives: Recently, a deuterated tracer, D6-[^{18}F]FP-(+)-DTBZ, 9-O-hexadeutero-3-[^{18}F]fluoropropoxyl-(+)-dihydrotetrabenazine ([^{18}F]**9**), targeting vesicular monoamine transporter 2 (VMAT2) in the central nervous system, was reported as a useful imaging agent for the diagnosis of Parkinson's disease (PD). The production of [^{18}F]**9** was optimized and simplified by using solid-phase extraction (SPE) purification.
Methods: Three major nonradioactive impurities were synthesized and characterized. The preparation of [^{18}F]**9** was optimized by using different labeling conditions, and an SPE purification method was evaluated. The influence of chemical impurities in the final dose of [^{18}F]**9** was assessed by an in vitro binding assay, an assay of the in vivo biodistribution in mice, and ex vivo and in vitro autoradiography of brain sections.
Results: Optimized fluorination conditions for [^{18}F]**9** were found – heating at 130 °C for 10 min in DMSO, and a high radiochemical yield and three major chemical impurities were observed. An SPE method involving a Sep-Pak® tC18 Plus Light cartridge with a two-step elution process was successfully implemented. This process gave a good radiochemical yield (38.7 ± 10.5%, decay corrected; radiochemical purity >99%) and low chemical impurities. An in vivo biodistribution study and autoradiography of brain sections showed that there was no significant difference between HPLC-purified and SPE-purified [^{18}F]**9**.
Conclusion: A VMAT2 targeting imaging agent, D6-[^{18}F]FP-(+)-DTBZ, [^{18}F]**9**, was prepared by optimized labeling conditions and an easy SPE purification. This method offers a short preparation time and operational simplicity. In conjunction with PET imaging, this new VMAT2 agent might be a useful clinical tool for diagnosing PD.

1. Introduction

Vesicular monoamine transporter 2 (VMAT2) plays an important role in neuronal transmission and is critical in the mechanism of the packing and storing of monoamine neurotransmitters in vesicles. Unlike the environment on the synaptic membrane, where there are specific and distinct transporters for the reuptake of three monoamines (dopamine, serotonin and norepinephrine), VMAT2 nonselectively transports all three monoamines from the cytosol into the vesicular lumen and it a common ATP-dependent transporter. The VMAT2 transporters are active only when VMAT2-containing neurons are active. Therefore, imaging VMAT2 in the brain can elucidate the neuronal integrity (total number) of all three monoaminergic neurons, which is important for understanding neurological and psychiatric disorders [1,2].

Tetrabenazine (TBZ, Xenazine), used to treat hyperkinetic movement disorders, was approved by the FDA in 2008 [3,4]. Relative to TBZ, its metabolite, dihydrotetrabenazine (DTBZ), showed higher biological stability and less sensitivity to drugs affecting dopamine levels in the brain. DTBZ has been labeled with the radionuclide ^{11}C, dihydrotetrabenazine ([^{11}C]-(+)-DTBZ), which was successfully applied in the diagnosis of Parkinson's disease (PD). However, the natural short half-life of ^{11}C ($T_{1/2}$ = 20 min) limits the widespread use of [^{11}C]-(+)-DTBZ [5–7]. An alternative VMAT2 binding agent, a 9-fluoropropoxyl derivative of dihydro-tetrabenazine ([^{18}F]FP-(+)-DTBZ, a.k.a. AV-133, florbenazine) labeled with ^{18}F, which has a longer half-life ($T_{1/2}$ = 110 min), has been successfully evaluated as a PET imaging agent for mapping VMAT2 in the brain. Clinical studies have suggested that [^{18}F]FP-(+)-DTBZ PET imaging is useful because the reduction in VMAT2 binding in the striatum is correlated with neuron deficits, which is valuable in the diagnosis of PD [8–13]. Neurodegeneration of dopamine neurons can be readily detected prior to the expression of PD symptoms, allowing early diagnosis [14–16]. [^{18}F]FP-(+)-

* Corresponding author at: Five Eleven Pharma Inc., Philadelphia, PA 19104, USA.
E-mail address: kunghf@gmail.com (H.F. Kung).

https://doi.org/10.1016/j.nucmedbio.2019.07.002
0969-8051/

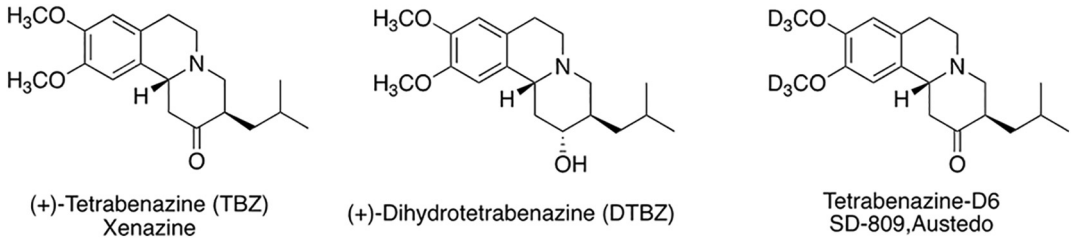

Fig. 1. Chemical structures of VMAT2 targeting agents: (+)-tetrabenazine (TBZ, Xenazine), (+)-dihydrotetrabenazine (DTBZ) and tetrabenazine-D6 (SD-809, Austedo).

DTBZ may be a useful biomarker for measuring dopaminergic degeneration in vivo and monitoring the severity of disease [17]. [^{18}F]FP-(+)-DTBZ shows a significant correlation between VMAT2 density and cognitive performance in patients with Lewy body dementia (DLB) [18].

Although [^{18}F]FP-(+)-DTBZ has demonstrated clinical utility and, potentially, can be used as a clinical tool to facilitate the diagnosis of PD, ten years after this agent was first tested in humans, it has not received FDA approval. Currently, there is no potential replacement for ^{18}F-labeled DTBZ for imaging VMAT2 binding sites in the brain. We developed a suitable "new chemical entity" – a deuterated DTBZ derivative, D6-[^{18}F]FP-DTBZ ([^{18}F]**9**), which was recently reported as an alternative VAMT2 imaging agent [19]. This new agent, which has "freedom of operation", can be commercially developed to assist in the diagnosis of PD by visualizing reductions in viable neurons in the basal ganglia regions of the brain.

Deuterium (D) is a stable isotope of hydrogen (H), providing a novel strategy for developing new drugs. The physical and chemical properties of deuterium are similar to those of hydrogen. Because carbon-deuterium (C-D) bonds are generally stronger than corresponding carbon hydrogen (C—H) bonds, selective deuterium substitution may lead to beneficial changes in the pharmacology and pharmacokinetics of drugs by decreasing their rate of metabolism [20–23]. Recently, the FDA has approved a deuterated derivative of TBZ, tetrabenazine-D6 (SD-809, Austedo, Fig. 1), for the treatment of Huntington's disease. Tetrabenazine-D6, in which two methyl groups have been substituted with deuterated methyl groups, provides improved drug efficacy [24]. Similarly, a deuterated derivative of D6-[^{18}F]FP-(+)-DTBZ, [^{18}F]**9**, has been prepared as a VMAT2 PET imaging agent (Fig. 2) [19]. After iv injection into rats, [^{18}F]**9** showed excellent regional brain signals for PET imaging of VMAT2 and improved plasma stability as demonstrated by a reduction in bone uptake due to defluorination [19].

One major issue of using D6-[^{18}F]FP-(+)-DTBZ, [^{18}F]**9**, for widespread clinical application is that its preparation required the use of semipreparative radio-HPLC. This relatively long and laborious process may be accompanied by considerable losses in the radioactive product. In the development of a method for the large-scale clinical use for [^{18}F]FDG, HPLC purification was replaced by solid-phase extraction (SPE). Multiple sequential solid-phase cartridges were adopted for hydrolysis of the protecting groups and the final purification. Since the 1990s, this simplified process for the preparation of [^{18}F]FDG has been the main process used for daily routine preparations of this compound [25–27]. In recent years, an increasing number of PET radiotracers have been purified by SPE. [^{18}F]FMZ ([^{18}F]Flumazenil, ethyl 8-fluoro-5,6-dihydro-5-methyl-6-oxo-4H-imidazo[1,5-a][1,4]benzodiazepine-3-carboxylate) [28], a well-known radioligand for assessing $GABA_A$ receptors, was synthesized based on a two-step SPE procedure. The SPE purification method for [^{18}F]FES ([^{18}F]Fluoroestradiol, 16α-fluoroestradiol-17β-sulfamate) [29], a radiotracer for diagnosing and monitoring the treatment of breast cancer, using Oasis Wax 3cc and Sep-Pak QMA light cartridges, afforded [^{18}F]FES in 15% RCY. Therefore, implementing radiolabeling and purification via SPE is a common tactic for simplifying purifications and improving yields.

Molar activity, particularly for neuroimaging, has a dramatic impact on PET imaging. Small amounts of nonradioactive chemicals (chemical byproducts) do not affect the specific distribution and binding. In the package inserts of FDA-approved neuroimaging agents, the recommended chemical doses for [^{18}F]AV-45 (florbetapir, Amyvid) and [^{18}F]AV-1 (florbetaben, Neuraceq) are "mass dose" no higher than 50 μg and 30 μg, respectively [30]. An SPE preparation of [^{18}F]FP-(+)-DTBZ was reported previously [31]. The report indicated that there was a significant amount of pseudocarrier (OH-derivative, 200–600 μg) remaining in the final dose. Although PET imaging studies in normal and unilaterally lesioned monkey brains showed no significant difference in striatal localization between HPLC- and SPE-purified [^{18}F]FP-(+)-DTBZ. Ex vivo inhibition studies suggested that the highest dose (3.5 mg/kg) of pseudocarrier (OH-derivative) via SPE purification might inhibit total binding by 20% [32].

Previously, the preparation of D6-[^{18}F]FP-(+)-DTBZ, [^{18}F]**9**, employed HPLC to remove the hydroxyl side product, which is produced after the hydrolysis of the O-tosylate (-OTs), **7**, to the corresponding hydroxyl derivative, **6** [19]. To reduce the preparation time and simplify the production process, we report herein a streamlined SPE process with a combination of ethanol-water as the eluent, and the majority of hydroxyl side product **6** and other related impurities were removed from the product using the developed method. Herein, we reduced the "mass dose" to no higher than 50 μg and confirmed that the amount of nonradioactive chemicals will not affect the specific distribution at low activity. This simplified SPE method might produce multiple doses of D6-[^{18}F]FP-(+)-DTBZ, [^{18}F]**9**, facilitating its widespread clinical application in the diagnosis of PD.

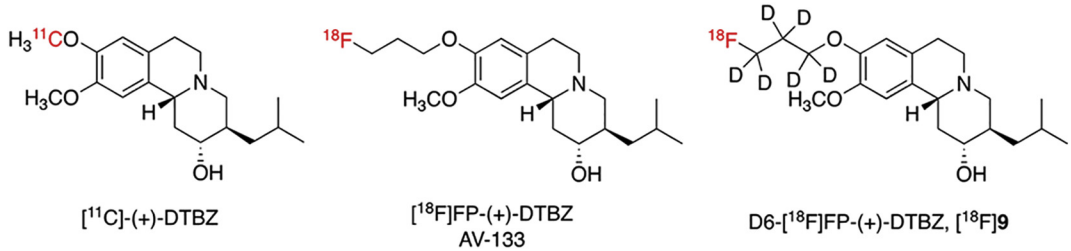

Fig. 2. Chemical structures of VMAT2 imaging agents: [^{11}C]-(+)-DTBZ and [^{18}F]FP-(+)-DTBZ (AV-133) and D6-[^{18}F]FP-(+)-DTBZ, [^{18}F]**9**.

2. Experimental section

2.1. General

All reagents were obtained commercially and used without further purification unless indicated. All deuterated chemicals were purchased from Toronto Research Chemicals Inc. Solvents were dried using a molecular sieve system (Pure Solve Solvent Purification System; Innovative Technology, Inc.). The ^{1}H NMR and ^{13}C NMR spectra were recorded on an Avance spectrometer at 400 and 100 MHz, respectively, and referenced to NMR solvents as indicated. High-resolution mass spectrometry (HRMS) data were obtained with an Agilent (Santa Clara, CA) G3250AA LC/MSD TOF system. Generally, crude compounds were purified by flash column chromatography (FC) over silica gel (Aldrich). All SPE cartridges used were purchased from Waters Corporation, USA, and Macherey-Nagel, Germany. Prior to use, Sep-Pak® Oasis HLB, Sep-Pak® tC2 Plus Light, Sep-Pak® C8 Plus Short, Sep-Pak® tC18 Plus Light, Sep-Pak® CN Plus Short, Chromafix C4, Chromafix C18 and Chromafix C18 Hydrawere cartridges were activated by flushing with 5 mL of ethanol followed by 10 mL of water. Sep-Pak Accell Plus QMA Light cartridges were activated with 10 mL of 0.5 M K_2CO_3 followed by 10 mL of water.

2.2. Chemistry

Initially, we planned to investigate the radiolabeling of desired D6-[^{18}F]FP-(+)-DTBZ, [^{18}F]**9**, following a previously reported procedure involving a direct S_N2 fluorination reaction (Scheme 1). By carefully examining the reaction, displacement of -OTs by fluoride anion, it was predicted that the reaction may lead to several side products. We reasoned that three side products would be produced by a. hydrolysis of the -OTs group, leading to the hydroxy side product (compound **6**); b. elimination leading to the vinyl side product (compound **3**); and c. the nucleophilic substitution of the phenol DTBZ (cleavage of the carbon chain from the phenolic hydroxy group at high temperature) by the -OTs precursor leading to the dimer side product (compound **8**). To fully investigate these possible side products, we carefully performed LC/MS analysis of the reaction mixture after the radiolabeling reaction, and the LC/MS results clearly showed the three expected side products listed above (Fig. S1A). All these side products were then synthesized for use as standards for validation and generating standard calibration curves for HPLC analysis (Scheme 2).

2.2.1. (2R,3R,11bR)-3-Isobutyl-10-methoxy-1,3,4,6,7,11b-hexahydro-2H-pyrido[2,1-a]isoquinoline-2,9-diol, (**1**)

A mixture of (2*R*,3*R*,11b*R*)-9-(benzyloxy)-3-isobutyl-10-methoxy-2,3,4,6,7,11b-hexahydro-2*H*-pyrido[2,1-*a*]isoquinolin-2-ol (1.59 g, 4 mmol) and 10% dry Pd/C (30 mg) was stirred in tetrahydrofuran (THF, 20 mL) and ethanol (EtOH, 20 mL) under H_2 at room temperature overnight. The reaction mixture was filtered and washed with EtOH (30 mL) and THF (30 mL). The solvent was removed under vacuum to give 1.18 g of compound **1** (yield 96%) as a yellow solid. ^{1}H NMR (400 MHz, $CDCl_3$) δ 6.68 (s,1H), 6.67 (s, 1H), 3.87 (s, 3H), 3.44–3.38 (m, 1H), 3.16–2.97 (m, 4H), 2.66–2.56 (m, 2H), 2.49–2.42 (m, 1H), 1.99 (t, J = 2.01 Hz, 1H), 1.79–1.68 (m, 2H), 1.57–1.45 (m, 3H), 1.12–1.05 (m, 1H), 0.97–0.93 (m, 6H). HRMS calcd. for $C_{18}H_{27}NO_3$ $[M + H]^+$ 306.1991, found 306.2100.

2.2.2. Allyl-d_5-4-methylbenzenesulfonate, (**2**)

To a suspension of sodium hydride (60% in mineral oil, 7 mg, 0.26 mmol) and ethyl ether (Et_2O 2 mL) under an argon atmosphere was added prop-2-en-d_5-1-ol (11 mg, 0.17 mmol) at room temperature. After gas evolution ceased, the reaction mixture was cooled to 0 °C. p-Toluenesulfonyl chloride (TsCl, 67 mg, 0.35 mmol) was dissolved in diethyl ether (Et_2O, 10 mL), and the resulting solution was slowly added to the reaction mixture. After the addition was complete, the reaction mixture was warmed to room temperature and allowed to stir for 3 h. The reaction mixture was added to a saturated solution of ammonium chloride (NH_4Cl, 10 mL) at 0 °C. Then, the mixture was extracted with ethyl acetate (EtOAc, 10 mL × 3). The combined the organic layer was dried over $MgSO_4$ and filtered. The filtrate was concentrated, and the residue was purified by FC (hexane/EtOAc = 85/15) to give 22.8 mg of compound **2** (yield: 62%) as a colorless oil. ^{1}H NMR (400 MHz, $CDCl_3$) δ 7.81–7.79 (m, 2H), 7.36–7.34 (m, 2H), 2.45 (s, 3H).

2.2.3. (2R,3R,11bR)-9-((Allyl-d_5)oxy)-3-isobutyl-10-methoxy-1,3,4,6,7,11b-hexahydro-2H-pyrido[2,1-a]isoquinolin-2-ol, (**3**)

To a mixture of compound **1** (30 mg, 0.1 mmol) in acetone (10 mL) was added compound **2** (22.8 mg, 0.1 mmol) followed by cesium carbonate (Cs_2CO_3, 130 mg, 0.4 mmol). The mixture was stirred at reflux for 2 h. After cooling to room temperature, 10 mL of water was added, and the mixture was extracted with ethyl acetate (EtOAc, 10 mL × 3). The combined the organic layer was dried over $MgSO_4$ and filtered. The filtrate was concentrated, and the residue was purified by FC (DCM/MeOH/$NH_3 \cdot H_2O$ = 95/5/0.5) to give 11 mg of compound **3** (yield 30%) as a yellow solid. ^{1}H NMR (400 MHz, $CDCl_3$) δ 6.50 (s, 1H), 6.41 (s, 1H), 3.66 (s, 3H), 3.24–3.19 (m, 1H), 2.99–2.83 (m, 4H), 2.46–2.39 (m, 2H), 2.31–2.26 (m, 1H), 1.83–1.78 (m, 2H), 1.57–1.52 (m, 2H), 1.43–1.32 (m, 2H), 0.91–0.85 (m, 1H), 0.77–0.73 (m, 6H). ^{13}C NMR (100 MHz, $CDCl_3$) δ 147.87, 146.69, 129.95, 126.55, 113.82, 108.55, 74.85, 61.12, 60.26, 56.25, 52.14, 41.86, 40.75, 39.89, 29.33, 25.57, 24.37, 21.97. HRMS calcd. for $C_{21}H_{26}D_5NO_3$ $[M + H]^+$ 351.2618 found 351.2706

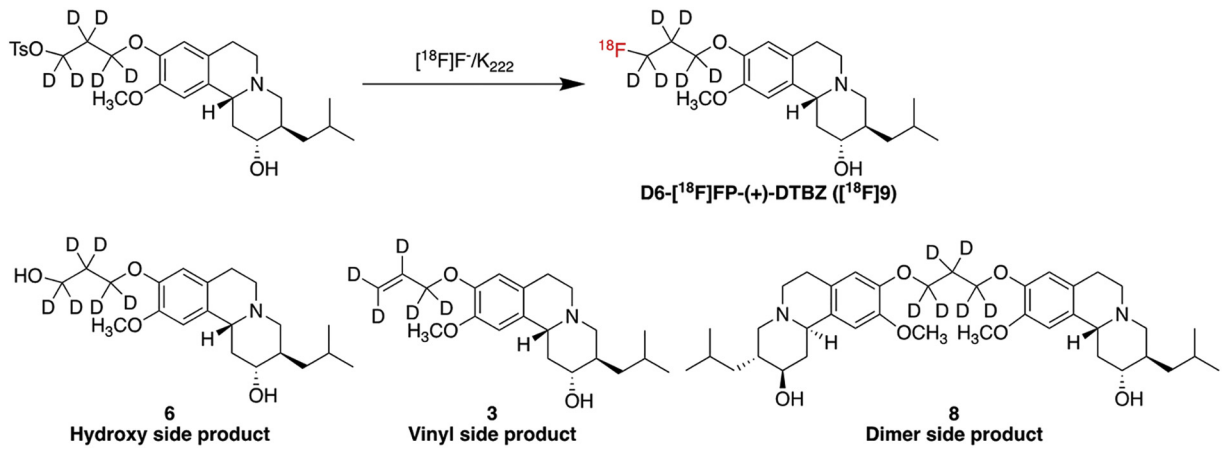

Scheme 1. Chemical reaction for the preparation of D6-[^{18}F]FP-(+)-DTBZ, [^{18}F]**9**, and the three chemical impurities, **3**, **6** and **8**, observed after [^{18}F]fluorination.

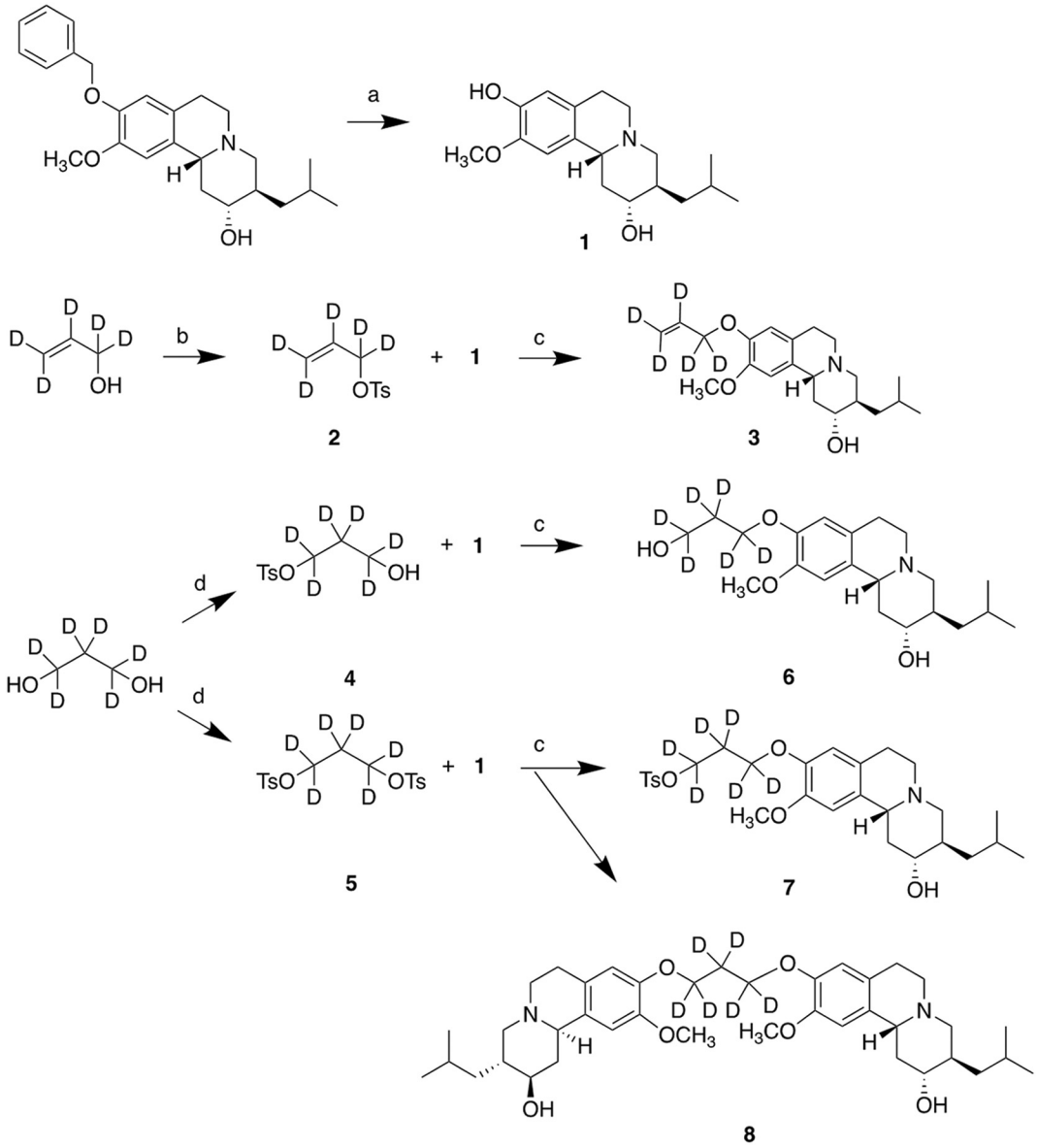

Scheme 2. Synthesis of compounds **3**, **6**, **7** (precursor) and **8**. a: Pd/C, H_2, EtOH/THF, rt, overnight; b: NaH, TsCl, Et_2O, 3 h, rt; c: Cs_2CO_3, acetone, reflux, 2 h; d: Et_3N, DMAP, TsCl, DCM, rt, overnight.

*2.2.4. 3-Hydroxypropyl-1,1,2,2,3,3-d_6 4-methylbenzenesulfonate, (**4**)*

To a solution of propane-d_6-1,3-diol (500 mg, 6.5 mmol) in dichloromethane (DCM, 10 mL) was added triethylamine (Et_3N, 888 mg, 8.8 mmol) and 4-dimethylaminopyridine (50 mg, 0.44 mmol). After the mixture was stirred at 0 °C for 10 min, a solution of p-toluenesulfonyl chloride (TsCl, 840 mg, 4.4 mmol) in DCM (20 mL) was added dropwise. After the addition was complete, the reaction mixture was warmed to room temperature and allowed to stir overnight. To the reaction mixture was added 15 mL of brine, and then it was extracted with DCM (10 mL × 3). The combined the organic layer was dried over $MgSO_4$ and filtered. The filtrate was concentrated, and the residue was purified by FC (hexane/EtOAc = 50/50) to give 500 mg of compound **4** (yield 50%) as a colorless oil. ^{1}H NMR (400 MHz, $CDCl_3$) δ 7.80–7.79 (m, 2H), 7.37–7.35 (m, 2H), 2.45 (s, 3H). ^{13}C NMR (100 MHz, $CDCl_3$) δ 145.09, 133.19, 130.11, 128.10, 21.87. HRMS calcd. for $C_{10}H_8D_6O_4S$ $[M + H]^+$ 237.0989 found 237.1022.

*2.2.5. Propane-1,3-diyl-d_6 bis(4-methylbenzenesulfonate), (**5**)*

Compound **5** was prepared from propane-d_6-1,3-diol (0.36 g, 4.46 mmol), triethylamine (Et_3N, 1.8 g, 18 mmol), 4-dimethylaminopyridine (61 mg, 0.5 mmol), p-toluenesulfonyl chloride (TsCl, 2.1 g, 11 mmol) and dichloromethane (DCM, 10 mL) following the same procedure described for compound **4**. FC with hexane/EtOAc (60/40) gave 1.56 g of compound **5** (yield 90%) as a white solid. ^{1}H NMR (400 MHz, $CDCl_3$) δ 7.78–7.76 (m, 4H), 7.38–7.36 (m, 4H), 2.48 (s, 6H). ^{13}C NMR (100 MHz, $CDCl_3$) δ 145.28, 132.85, 130.18, 128.10, 21.88. HRMS calcd. for $C_{17}H_{14}D_6O_6S_2$ $[M + H]^+$ 391.1078. found 391.1140.

*2.2.6. (2R,3R,11bR)-9-(3-Hydroxypropoxy-1,1,2,2,3,3-d_6)-3-isobutyl-10-methoxy-1,3,4,6,7,11b-hexahydro-2H-pyrido[2,1-a]isoquinolin-2-ol, (**6**)*

Compound **6** was prepared from compound **1** (50 mg, 0.16 mmol), compound **4** (50 mg, 0.2 mmol), cesium carbonate (Cs_2CO_3, 208 mg, 0.64 mmol) and acetone (15 mL) following the same procedure described for compound **3**. The concentrated residue was purified by FC (DCM/MeOH/$NH_3 \cdot H_2O$ = 90/9/1) to give 30 mg of compound **6** (yield 52%) as a pale-yellow solid. ^{1}H NMR (400 MHz, $CDCl_3$) δ 6.69 (s, 1H), 6.63 (s, 1H), 3.82 (s,3H), 3.48–3.40 (m, 1H), 3.16–3.03 (m, 4H), 2.65–2.57 (m, 2H), 2.47 (t, J = 1.6 Hz, 1H), 2.02–1.97 (m, 1H), 1.71–1.75 (m, 2H), 1.63–1.49 (m, 2H), 1.07–1.12 (m, 1H), 0.95–0.97

(m, 6H). ^{13}C NMR (100 MHz, $CDCl_3$) δ 147.70, 146.71, 130.02, 126.49, 113.59, 108.29, 74.55, 60.93, 60.06, 55.97, 51.83, 41.57, 40.52, 39.69, 29.07, 25.37, 24.11, 21.77. HRMS calcd. for $C_{21}H_{27}D_6NO_4$ $[M + H]^+$ 370.2786 found 370.3505.

*2.2.7. 3-(((2R,3R,11bR)-2-Hydroxy-3-isobutyl-10-methoxy-1,3,4,6,7,11b-hexahydro-2H-pyrido[2,1-a]isoquinolin-9-yl)oxy)propyl-1,1,2,2,3,3-d_6 4-methylbenzenesulfonate, (**7**)*

Compound **7** was prepared from compound **1** (100 mg, 0.33 mmol), compound **5** (140 mg, 0.35 mmol), cesium carbonate (Cs_2CO_3, 427 mg, 1.3 mmol) and acetone (30 mL) following the same procedure described for compound **3**. The concentrated residue was purified by FC (DCM/MeOH/$NH_3 \cdot H_2O$ = 95/5/0.5) to give 100 mg of compound **7** (yield 58%) as a pale-yellow solid. ^{1}H NMR (400 MHz, $CDCl_3$) δ 7.78–7.75 (m, 2H), 7.25–7.27 (m, 2H), 6.66 (s, 1H), 6.51 (s, 1H), 3.77 (s, 3H), 3.39–3.38 (m, 1H), 3.13–2.99 (m, 4H), 2.63–2.56 (m, 2H), 2.47–2.40 (m, 4H), 2.00–1.95 (m, 1H), 1.70–1.72 (m, 2H), 1.53–1.48 (m, 2H), 1.13–1.15 (m, 1H), 0.96–0.94 (m, 6H). ^{13}C NMR (100 MHz, $CDCl_3$) δ 147.80, 146.80, 130.00, 126.61, 113.79, 108.76, 74.58, 60.91, 60.08, 56.15, 51.88, 41.62, 40.55, 39.70, 29.10, 25.36, 24.12, 21.78. HRMS calcd. for $C_{39}H_{52}D_6N_2O_6$ $[M + H]^+$ 524.2875 found 524.2927.

*2.2.8. (2R,2′R,3R,3′R,11bR,11b'R)-9,9′-((Propane-1,3-diyl-d_6)bis(oxy))bis(3-isobutyl-10-methoxy-1,3,4,6,7,11b-hexahydro-2H-pyrido[2,1-a]isoquinolin-2-ol), (**8**)*

The residue from the synthesis of compound **7** was purified by FC (DCM/MeOH/$NH_3 \cdot H_2O$ = 90/9/1) to give 5.8 mg of compound **8** (yield 5%) as a pale-yellow solid. ^{1}H NMR (400 MHz, $CDCl_3$) δ 6.67–6.34 (m, 2H), 3.81 (s,6H), 3.39–3.43 (m, 2H), 3.15–2.99 (m, 8H), 2.62–2.59 (m, 4H), 2.48–2.43 (m, 2H), 1.99 (t, J = 10.8, 2H), 1.73–1.63 (m, 4H), 1.63–1.46 (m, 6H), 1.46–1.03 (m, 2H), 0.97–0.93 (m, 12H). ^{13}C NMR (100 MHz, $CDCl_3$) δ 147.88, 147.14, 129.81, 126.67, 113.84, 108.67, 74.85, 61.10, 60.24, 56.29, 52.05, 41.78, 40.74, 39.90, 29.28, 25.55, 24.37, 21.98. HRMS calcd. for $C_{39}H_{52}D_6N_2O_6$ $[M + H]^+$ 657.4671 found 657.4100.

2.3. Nucleophilic [^{18}F]fluorination of 9 under different conditions

A solution containing [^{18}F]fluoride (37–74 MBq) was loaded onto an activated QMA light cartridge and eluted with 1 mL of K_{222}/K_2CO_3 solution (2 mg K_2CO_3, 10 mg K_{222} in 0.15 mL of water and 0.85 mL of acetonitrile) into a glass test tube. The solution was dried under a flow of argon at 90 °C and azeotropically dried with 2 mL of acetonitrile. The precursor (1 mg) was dissolved in 1 mL of solvent (DMSO, DMF, DMA or ACN) and added to the dried [^{18}F]$F^-/K_{222}/K_2CO_3$ complex. The reaction mixture was heated to different temperatures (70 °C, 75 °C, 90 °C, 110 °C or 130 °C). Aliquots (20 μL) were removed at different time points (5, 10 and 15 min), and the aliquots were quenched in ice water prior to analysis by HPLC.

2.4. Analysis of the radiochemical yield, radiochemical purity and amount of chemicals by HPLC

The radiochemical yield (RCY) and radiochemical purity (RCP) were analyzed by HPLC with a gamma ray radio detector and a UV/Vis detector (Agilent 1200 series, Ascentis C18 column, 150 × 4.6 mm; 280 nm) with the following mobile phase (1 mL/min) gradient. From 0 to 2 min, isocratic 10 mM ammonium formate buffer (AFB) 95%, ACN 5%; from 2 to 5 min, gradient AFB 95–30%, ACN 5–70%; from 5 to 10 min, gradient AFB 30–0%, ACN 70–100%; from 10 to 15 min, gradient AFB 0–95%, ACN 100–5%; and from 15 to 20 min, 95% AFB (retention times: [^{18}F]fluoride = 1.4 min, [^{18}F]**9** = 7.8 min). The amounts of compounds **3, 6, 7,** and **8** were quantified using this HPLC system; standard calibration curves were plotted using authentic sample solutions at least 6 different concentrations from 0.01 μg to 1 μg (Fig. S1B).

The samples were analyzed by LC/MS with an Agilent LC/MSD TOF instrument in positive ESI mode and an Agilent HPLC 1100 series system. The HPLC conditions were as follows: stationary phase: Agilent Poroshell 120 EC-C18 2.7 μ 3.0 × 50 mm; mobile phase: 0.4 mL/min: UV detection: 280 nm; and ESI positive mode. The following gradient was used: from 0 to 15 min, gradient 0.1% formic acid 100–0%, ACN 0–100%; and from 15 to 20 min, 100% ACN.

2.5. Solid-phase extraction (SPE) purification

The reaction mixture was cooled to room temperature, and 7 mL of water was added. The mixture was loaded onto different cartridges (eight different cartridges were tested: Sep-Pak Oasis, tC2, C8, tC18, CN, Chromafix C18 Hydrox, Chromafix C18, and Chromfix C4). The loaded cartridges were first washed with 10 mL of water and then eluted with 2 mL of gradient concentrations of ethanol-water or acetonitrile-water (10%, 20%, 30%, 40%, 50% and 60%). The resulting eluates were analyzed by HPLC. To optimize the elution volume, the selected cartridges were washed with water, followed by different concentrations (25%, 30% or 35%) of ethanol-water in 2 mL portions. The flow rate was approximately 10 mL/min.

2.6. Semipreparative HPLC purification method

The reaction mixture was cooled to room temperature, and 7 mL of water was added to this mixture. The mixture was loaded onto an Oasis HLB (3 cc) cartridge and then washed with 10 mL of water. [^{18}F]**9** was eluted with 1 mL of acetonitrile. This solution was diluted with 1 mL of 10 mM AFB and injected into the HPLC system (Gemini 250 × 10 mm, ACN/10 mM AFB = 45/55, 3 mL/min). The eluate from 14.0 to 15.5 min was collected and diluted with 25 mL of water. This mixture was loaded onto a tC18 cartridge, from which the desired product, [^{18}F]**9**, was eluted with 1 mL of ethanol.

2.7. In vitro binding assay for IC_{50} determination

Tissue homogenates of striatum (dissected from mouse brain) were prepared in buffer 1 (50 mM of HEPES, 0.32 M sucrose, pH = 7.4). Compounds were examined for their ability to compete with [^{18}F]**9** for binding at concentrations ranging from 10^{-6} to 10^{-11} M. The binding assays were performed in glass tubes (12 × 75 mm) with final volumes of 0.25 mL. In the nonspecific binding assay, 50 μM (±)-tetrabenazine (TBZ), was used as the positive control. After incubation for 1 h at room temperature, the bound ligand was separated from the free ligand by filtration through glass fiber filters. The filters were washed three times with 4 mL of ice-cold PBS buffer at pH 7.4, and the radioactivity of the material remaining on the filters was counted with a gamma counter (WIZARD^2, Perkin-Elmer). Data were analyzed using the nonlinear least-square curve fitting program LIGAND to determine IC_{50} values.

2.8. In vivo biodistribution in mice

Five normal CD-1 mice per group were used for each biodistribution study. The assay used 0.15 mL of solutions containing different concentrations of **3**, **6**, and **8**. HPLC-purified [^{18}F]**9** in 0.1% bovine serum albumin was injected into the tail vein of CD-1 mice (33–37 g, male) while they were under isoflurane anesthesia (1.11 MBq per mouse). The mice (n = 5) were sacrificed by cervical dislocation at 30 min postinjection. The organs or tissues of interest were removed and weighed, and radioactivity was counted with an automatic gamma counter. The percentage of the dose per organ was calculated by comparing the tissue counts with suitable diluted aliquots of the injection material. Different regions of the brain corresponding to the cerebellum (CB), striatum (ST), hippocampus and cortex were dissected from the brains and counted separately.

2.9. Ex vivo autoradiography

Two normal CD-1 mice were injected with HPLC- or SPE-purified 18.5 MBq [^{18}F]**9** via the tail vein and sacrificed at 30 min postinjection. The brain of each mouse was harvested and frozen. Coronal sections 20 μm thick were cut on a cryostat, thaw-mounted onto slides and dried at room temperature. The dried sections were exposed to imaging plates for 30 min, and images were acquired using a Typhoon FLA 7000 (GE Healthcare Life Sciences).

2.10. In vitro autoradiography

All 20-μm-thick coronal sections of rats and monkeys were stored at −20 °C until use in vitro autoradiography. Prior to the assays, the sections were thawed, dried at room temperature and preincubated for 20 min in an ice-cold incubator. The assay was then carried out in Coplin jars in ice-cold incubation buffer 1 for 15 min at room temperature. [^{18}F]**9** was diluted in buffer 1 to yield approximately 30,000 CPM/mL, and compounds **3**, **6** and **8** were diluted in buffer 1 to 5.7 nmol/mL, 2.7 nM/mL and 6.0 nM/mL, respectively. The brain sections were incubated at room temperature for 30 min with 1 mL of [^{18}F]**9** solution and then rinsed with PBS twice and water for 3 min. The sections were dried and then exposed to imaging plates for 30 min.

3. Results and discussion

3.1. Optimization of the ^{18}F fluorination conditions

The fluorination reaction for the preparation of [^{18}F]FP-(+)-DTBZ, [^{18}F]**9**, is an S_N2 reaction with an O-tosyl leaving group in which the [^{18}F]fluoride ion is activated by complexing with K^+/K_{222}. Three parameters of this fluorination were investigated to maximize the RCY: the solvent, reaction time and reaction temperature. The reaction was performed in 1 mL of DMF, DMA or DMSO solution containing 1 mg (1.9 μmol) of compound **7** at 110 °C for 10 min. This labeling reaction was also performed in 1 mL of ACN at 75 °C for 10 min in a closed vial (due to the lower boiling point of ACN). As shown in Table 1, when the labeling was performed in DMF, DMA, ACN and DMSO, the RCYs were 50.7%, 14.3%, 73.0% and 79.0%, respectively. Fluorination in DMSO at 110 °C for 10 min provided the highest RCY (79%); therefore, subsequent reactions were all carried out in DMSO.

The effects of temperature and time in the production of D6-[^{18}F]FP-(+)-DTBZ, [^{18}F]**9**, were evaluated in DMSO as the solvent. The RCYs improved with increasing temperature; the RCYs in DMSO for 5 min were 52%, 71%, 79%, and 88% at 70 °C, 90 °C, 110 °C and 130 °C, respectively (Table 2). The labeling yield did not improve significantly with a longer heating time, suggesting that the S_N2 fluorination reaction was complete in 10 min. Additionally, the RCYs decreased with longer heating times (15 min), suggesting that more side reactions occurred.

The time and temperature of the fluorination reaction in DMSO were further optimized. Initially, the goal was to maximize the labeling yield of D6-[^{18}F]FP-(+)-DTBZ, [^{18}F]**9**, and reduce or eliminate the remaining OTs-precursor, **7**. At a higher temperature, the amount of OTs- precursor **7** remaining was below the detection limit, which simplified the subsequent SPE purification. The amounts of all chemicals in the crude mixture from the fluorination reaction were analyzed by HPLC compared with the calibration curves of authentic samples (Fig. S1). Three major chemical products were produced in the reaction mixture: the OH–side product, **6**; the OTs-precursor, **7**; and the dimer side product, **8**

Table 1
Fluorination reactions in different solvents at different temperatures for producing D6-[^{18}F]FP-(+)-DTBZ, [^{18}F]**9**. (Avg ± SD, n = 3).

Solvent[a]	Time (min)	Temp. (°C)	RCY[b] (%)
DMF	10	110	50.7 ± 13.6
DMA	10	110	14.3 ± 1.20
ACN	10	75	73.0 ± 6.90
DMSO	10	110	79.0 ± 3.90

[a] DMA = *N*,*N*-dimethylacetamide; DMF = *N*,*N*-dimethylformamide; ACN = acetonitrile; DMSO = dimethyl sulfoxide.
[b] Determined by radio-HPLC analysis of the crude product.

Table 2
Results of the fluorination reaction for producing D6-[^{18}F]FP-(+)-DTBZ, [^{18}F]**9**, in DMSO at different temperatures and times. The goal was to produce the highest RCY and the lowest amount of O-tosylated precursor, **7**. (Avg ± SD, n = 3).[a]

Time (min)	Temp. (°C)	RCY (%)	**6** (μg)	**8** (μg)	**7** (μg) (precursor)
5	70	52.0 ± 14.7	383 ± 123	50.1 ± 15.4	230 ± 206
10	70	52.7 ± 12.3	415 ± 69.4	49.6 ± 7.48	82.2 ± 142
15	70	56.3 ± 15.9	465 ± 57.4	56.7 ± 2.56	51.7 ± 89.5
20	70	49.3 ± 14.0	503 ± 19.3	58.1 ± 9.08	20.2 ± 35.1
5	90	71.3 ± 15.0	364 ± 48.7	109 ± 22.1	97.7 ± 132
10	90	69.0 ± 21.7	354 ± 112	120 ± 44.4	12.9 ± 22.3
15	90	68.7 ± 19.9	411 ± 28.6	135 ± 25.3	0.00 ± 0.00
5	110	79.3 ± 4.90	305 ± 25.6	175 ± 18.1	0.00 ± 0.00
10	110	79.0 ± 3.90	354 ± 20.1	186 ± 6.72	0.00 ± 0.00
15	110	78.7 ± 3.50	370 ± 7.10	187 ± 11.2	0.00 ± 0.00
5	130	88.3 ± 5.80	358 ± 29.4	205 ± 23.5	0.00 ± 0.00
10	130	89.7 ± 6.60	357 ± 29.3	195 ± 17.1	0.00 ± 0.00
15	130	81.0 ± 7.50	395 ± 60.4	196 ± 17.2	0.00 ± 0.00

[a] Aliquots (10 μL) were removed from the reaction mixture at different time points (5, 10 and 15 min) were quenched in ice water. The RCYs and chemical impurities were determined by HPLC.

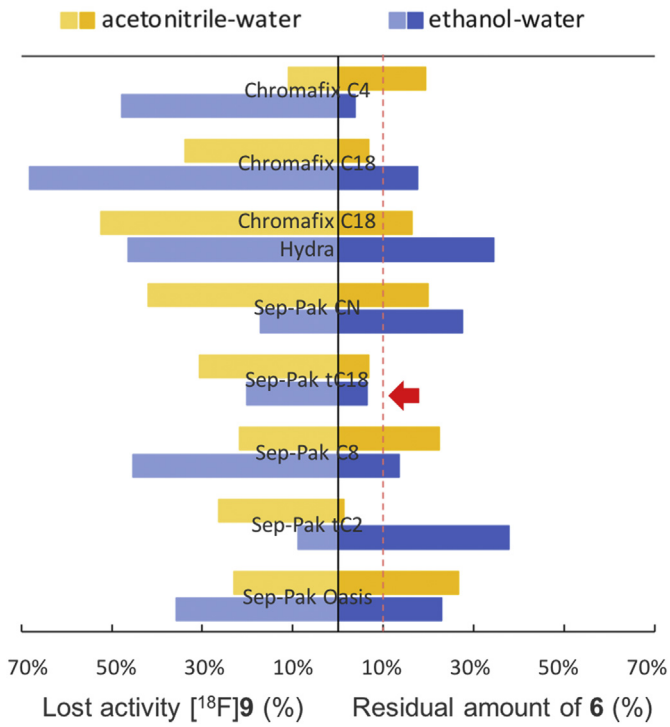

Fig. 3. Results of the initial SPE purifications using different cartridges to remove hydroxyl side product **6** and retain the desired product, [^{18}F]FP-(+)-DTBZ, [^{18}F]**9**. Eight different cartridges were tested (Sep-Pak Oasis, tC2, C8, tC18, CN, Chromafix C18 Hydrox, Chromafix C18, and Chromfix C4). After loading the crude ^{18}F-labeled reaction mixture on the cartridges, they were eluted with 2 mL of incremental concentrations ethanol-water and acetonitrile-water mixtures. The goal was to maximize the removal of residual hydroxyl side product **6** and retain the desired product, D6-[^{18}F]FP-(+)-DTBZ, [^{18}F]**9**. The initial evaluation suggested that tC18 most effectively removed hydroxyl side product **6** and retained the desired product (solid arrow indicates the best performance).

(Table 2). The residual OTs-precursor, **7**, was completely hydrolyzed and transformed into hydroxyl side product **6** and dimer side product **8** when the reaction was heated above 90 °C. More dimer side product **8** was produced at higher temperatures. This dimeric side product, **8**, derived from the fluorination of the O-tosyl-proproxy-phenyl group has not been reported in the literature. It is likely that a similar dimeric side product might have been produced in other similar reactions (the fluorination of O-tosyl-proproxy-phenyl groups). Since this type of fluorinated PET tracer is quite common in the field, one may wonder how often this type of side product was produced but not investigated or reported. By careful examination of the LC/MS data, another side product, vinyl derivative **3**, was found in the reaction mixture. The amount of vinyl derivative **3** was within the detection range; however, the total amount of **3** in the reaction mixture was extremely low (< 0.5 μg), which is often below the detection limit. All of these side products were authentically prepared and characterized. Based on the results listed in Table 2, DMSO was selected as the optimal solvent, and the reaction was heated at 130 °C for 10 min. The resulting crude reaction mixture was optimized via SPE purification.

3.2. SPE purification for the production of [^{18}F]**9**

Currently, "HPLC-free" purifications utilizing disposable SPE cartridges are widely used in PET radiochemistry. An SPE purification of [^{18}F]FP-(+)-DTBZ, [^{18}F]**9**, has been reported [31]. However, the reported SPE purification did not eliminate nonpolar chemical impurities, such as the hydroxyl side product. The final dose contained 200–600 μg of the pseudocarrier, 9-OH-DTBZ. Different cartridges and eluents were tested in the optimization of the SPE purification of D6-[^{18}F]FP-(+)-DTBZ, [^{18}F]**9**. The optimization had three objectives: achieve excellent radiochemical purity, maximize the radiochemical yield and minimize residual chemical impurities.

3.2.1. Gradient elution on different cartridges

Building on the reported SPE purification method for the preparation [^{18}F]FP-(+)-DTBZ, we aimed to reduce the major side product, hydroxyl side product, **6**. The choice of SPE cartridge was determined by the difference in the lipophilicities of [^{18}F]**9** and hydroxyl side product **6**. Therefore, we only selected and evaluated reversed-phase SPE cartridges. The fluorination was carried out using the optimized conditions described above (DMSO as the solvent, heating at 130 °C for 10 min). After cooling to room temperature, the crude reaction mixture (approximately 1 mL) was diluted with 7 mL of water and loaded onto different cartridges. Then, 2 mL portions of eluent (from 10% to 60% acetonitrile-water or ethanol-water) were used to elute the products. The purpose of this gradient elution was to find the suitable eluent concentration range when the majority of **6** was removed while retaining the desired product, [^{18}F]FP-(+)-DTBZ, [^{18}F]**9**, on the cartridge (Fig. 3; more detailed graphs are shown in Fig. S2). When the amount of residual **6** was <10% (red dotted line), the losses in activity of [^{18}F]**9** were 26.4%, 20.1%, 30.6%, 33.9% and 47.8% in Sep-Pak tC2 acetonitrile-water elution, Sep-Pak tC18 ethanol-water elution, Sep-Pak tC18 acetonitrile-water elution, Chromafix C18 acetonitrile-water elution and Chromafix C4 ethanol-water elution, respectively. We focused on Sep-Pak tC18 with ethanol-water elution and optimized the concentration and volume as this system showed the smallest loss in activity (Fig. 3, solid red arrow indicates the best combination).

3.2.2. Gradient elution and volume tests with the tC18 cartridge

Since the tC18 cartridge most effectively removed hydroxyl side product **6** and retained the desired product, [^{18}F]**9**, additional

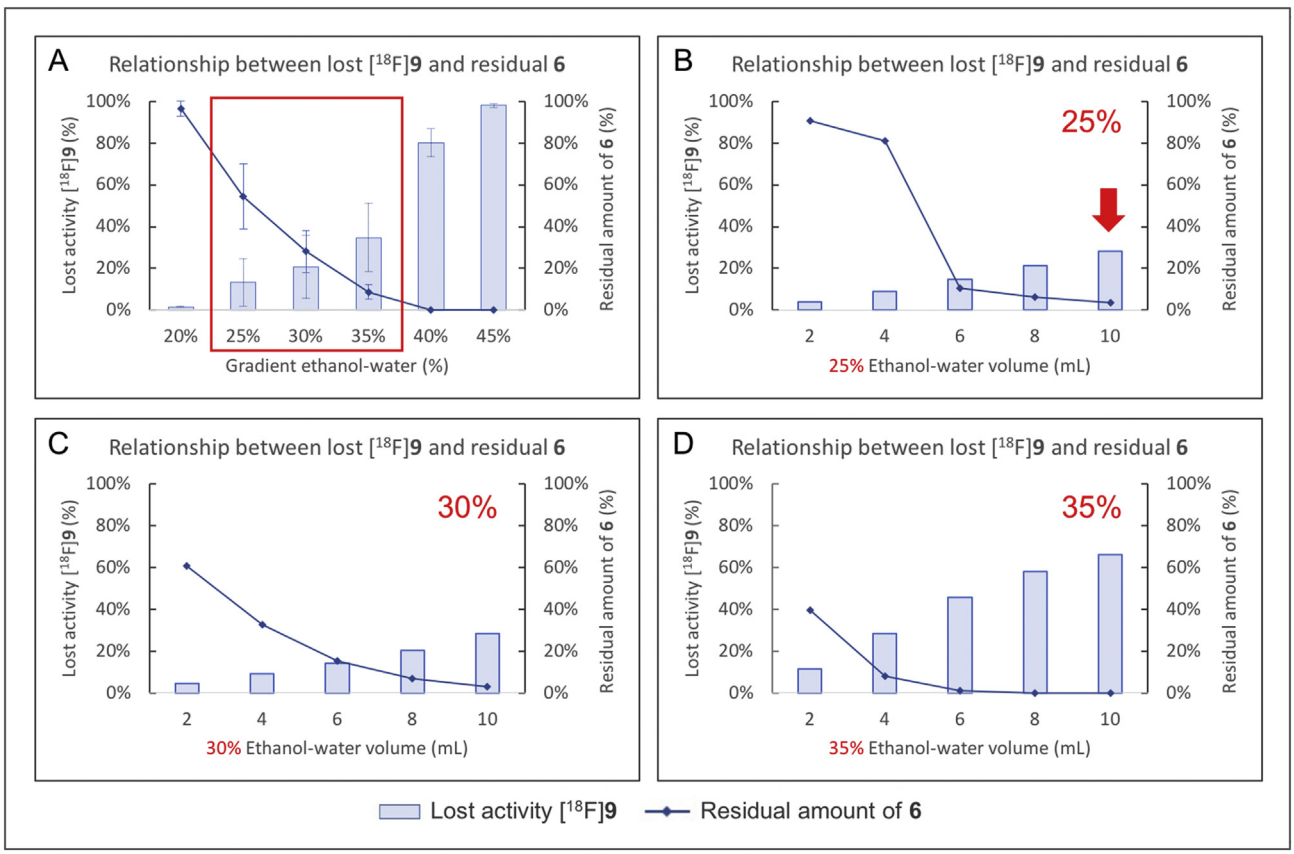

Fig. 4. Further refinement using an Sep-Pak tC18 cartridge to remove hydroxyl side product **6** and retain the desired product, [^{18}F]**9**, by using different ratios of ethanol-water as the eluent. A: Eluted with 2 mL portions of incremental concentrations of ethanol-water. B, C and D: Eluted with 2 mL portions of incremental concentrations of ethanol-water at 25%, 30% and 35%, respectively.

Table 3
Results of the optimized production of D6-[^{18}F]FP-(+)-DTBZ, [^{18}F]**9**, and the residual amounts of chemical impurities per batch (Avg ± SD, n = 9).[a]

Radiochemical yield, RCY (%)[b]	38.7 ± 10.5
Radiochemical purity, RCP (%)	>99%
Residual amount of **6**	34.7 ± 12.8 μg
Residual amount of **8**	4.36 ± 4.86 μg
Residual amount of **3**	< 0.5 μg

[a] The optimal conditions for the SPE purification were loading the crude fluorination reaction mixture on a Sep-Pak tC18 cartridge and eluting with 10 mL of 25% ethanol-water followed by 2 mL of 50% ethanol-water to give the final product, D6-[^{18}F]FP-(+)-DTBZ, [^{18}F]**9**.
[b] RCY (%) = activity of product/initial activity (%) (with decay correction).

optimization experiments were performed. Using ethanol-water mixtures ranging from 25%, 30% and 35% led to good results (Fig. 4A). After multiple experiments, 10 mL of 25% ethanol-water eluent was chosen for the first stage of the elution (solid red arrow, Fig. 4B). Under these conditions, dimer side product **8** was retained on the cartridge due to its high lipophilicity. Using 2 mL of 50% ethanol-water for the second stage of the elution produced the highest (89.1%) yield of the desired product, D6-[^{18}F]FP-(+)-DTBZ, [^{18}F]**9**, accompanied by 34.7 ± 12.8 μg of hydroxyl side product **6** and 4.36 ± 4.86 μg of dimer side product **8** (see Table 3).

The optimal conditions for SPE purification were finally selected: loading the crude fluorination reaction mixture to a Sep-Pak tC18 cartridge and eluting with 10 mL of 25% ethanol-water and then with 2 mL of 50% ethanol-water to give the final product, D6-[^{18}F]FP-(+)-DTBZ, [^{18}F]**9**. With these optimized conditions, the desired product, D6-[^{18}F]FP-(+)-DTBZ, [^{18}F]**9**, was obtained in 35 min with an average radiochemical yield, RCY, of 38.7 ± 10.5% (decay corrected, Avg ± SD, n = 9) and a radiochemical purity, RCP, of >99% (Table 3). There was a significant reduction in the impurities during the SPE purification (for the HPLC profiles before and after purification, see Fig. S3). This SPE purification method took only 5 min and resulted in an activity loss of 25.8 ± 16.4%. The activity lost in the HPLC purification method was 25.8 ± 16.4% (with decay correction), and it was a 30 min process. The activity losses with the SPE and HPLC purification methods were similar, but the SPE method was fast and simple.

Currently, the preparation has only been carried out at a radioactivity level of 37–370 MBq in the laboratory. For clinical applications in hospitals or radiopharmacies, the method should be automated in a hot cell and conducted at a higher radioactivity level (>37 GBq; sufficient for multiple patient doses).

3.3. In vitro binding assay

Using [^{18}F]**9** as the "hot" ligand and homogenates of striatum (dissected from mouse brain), the binding affinities of (±)-TBZ, FP-(+)-DTBZ, (AV-133), hydroxyl side product **6**, vinyl side product **3**, dimer side product **8** and "cold" D6-FP-(+)-DTBZ **9** were measured (Table 4). The results suggested that the binding affinities of deuterated AV133 and nondeuterated AV133 were similar (IC_{50} = 7.23 ± 0.20 and 3.24 ± 1.57 nM, respectively). Both showed higher binding affinity than (±)-TBZ. Among all the chemical impurities, **3** showed a comparably high binding affinity, whereas **6** and **8** showed much lower binding affinities. The results suggested that the impurity profile was very favorable. The impurity with the highest binding affinity, **3** (IC_{50} = 2.70 ± 0.56 nM), was not detectable below <0.5 μg per batch. The other impurities, **6** and **8**, which were present in higher quantities, showed hundred- or thousand-fold lower binding affinities for VMAT2 binding sites; therefore, they are unlikely to affect the binding of VAMT2 in vivo.

3.4. Biodistribution study in normal mice

To explore the potential effects of chemical impurities (compounds **3**, **6** and **8**) in the binding of [^{18}F]**9** (the final product) to VMAT2 in the brain, different concentrations of impurities were added to [^{18}F]**9** (purified by HPLC), and the solutions were tested in normal mice. In these injections, the average amounts of **6** and **8** in the SPE-purified product were 35 μg and 5 μg (Table 3), and the amount of **3** was <0.5 μg. The amounts of chemical impurities were estimated on a moles per kg basis from human to mouse by the following formula: (Human equivalent dose, HED, assumes that the average human weight is 70 kg and the average weight of a mouse is 35 g) [33].

$$\text{HED (mg/kg)} = \text{animal dose in mg/kg} \times (\text{animal weight in kg/human weight in kg})^{0.33}$$

Therefore, the amounts of **3**, **6** and **8** for mice were 8.6×10^{-5} mg/kg, 6.1×10^{-3} mg/kg and 8.6×10^{-4} mg/kg, respectively. We prepared mixtures with 10×, 100× and 1000× higher doses of **3**, **6** and **8** and added them to the HPLC-purified D6-[^{18}F]FP-(+)-DTBZ, [^{18}F]**9**. HPLC-purified [^{18}F]**9** without added chemical impurities was used as the control dose. Whole body and brain distribution in mice were evaluated using the doses listed above (Table 5). The results of the biodistribution study showed that there was no difference between the control (no added chemical impurities) and the 10× group. The 100× and 1000× groups showed a significant reduction in brain uptake. Comparing the 10× group and the control, there was no significant difference in regional brain distribution, i.e., striatum, cerebellum and cortex. Differences were observed between the 1000× group and the control in the pancreas ($p < 0.05$) and brain distribution (cerebellum $p < 0.05$; striatum, hippocampus, cortex and hypothalamus $p < 0.01$). It appears that the 10-fold higher content of chemical impurities in the final product did not influence the striatum uptake where VMAT2 binding sites are

Table 4
Comparison of in vitro binding affinities (IC_{50}, nM) of (±)-TBZ, FP-(+)-DTBZ (AV-133), D6-FP-(+)-DTBZ, **9** and other impurities (**3**, **6** and **8**) for vesicular monoamine transporter 2 (VMAT2).[a]

Compound	Structure	IC_{50} (nM) (Avg ± SD, n = 3)
(±)-Tetrabenazine	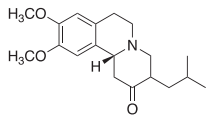	21.2 ± 1.74
FP-(+)-DTBZ (AV-133)	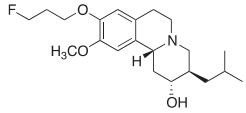	3.24 ± 1.57
D6-FP-(+)-DTBZ, **9**	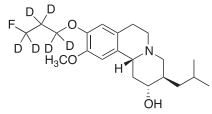	7.23 ± 0.20
3	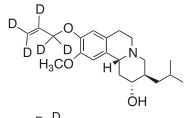	2.70 ± 0.56
6	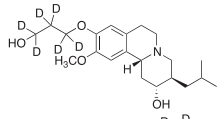	792 ± 113
8	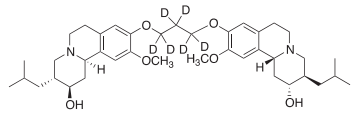	1341 ± 62.0

[a] In vitro binding studies were performed using mouse striatum homogenates, and the radio tracer was D6-[^{18}F]FP-(+)-DTBZ ([^{18}F]**9**) purified by HPLC (all chemical impurities were removed).

Table 5
Biodistribution of D6-[^{18}F]FP-(+)-DTBZ, [^{18}F]**9**, in normal mice at 30 min postinjection: a comparison of different amounts of added chemical impurities.[a] (n = 5, Avg ± SD).

	0×	10×	100×	1000×
Organ				
Blood	1.19 ± 0.16	1.56 ± 0.45	1.22 ± 0.16	1.52 ± 0.24
Heart	1.90 ± 0.18	1.93 ± 0.08	1.89 ± 0.10	1.89 ± 0.14
Muscle	1.22 ± 0.50	0.99 ± 0.10	0.98 ± 0.04	0.99 ± 0.07
Lung	2.52 ± 0.20	2.50 ± 0.18	2.38 ± 0.16	2.44 ± 0.21
Kidney	3.06 ± 0.37	3.32 ± 0.24	3.27 ± 0.33	3.56 ± 0.53
Spleen	3.34 ± 1.07	2.90 ± 0.26	2.67 ± 0.12	2.36 ± 0.46
Pancreas	15.2 ± 2.61	15.2 ± 1.00	15.6 ± 2.19	12.3 ± 0.98
Liver	10.5 ± 0.76	11.6 ± 0.71	12.7 ± 0.74	12.5 ± 0.93
Skin	1.34 ± 0.25	1.17 ± 0.09	1.23 ± 0.09	1.19 ± 0.05
Bone	2.28 ± 0.40	2.17 ± 0.42	2.28 ± 0.33	2.80 ± 0.22
Brain	2.11 ± 0.28	2.32 ± 0.25	1.85 ± 0.09	1.07 ± 0.06
Regional brain distribution				
Cerebellum	1.16 ± 0.14	1.30 ± 0.09	1.24 ± 0.10	0.94 ± 0.08
Striatum	5.19 ± 0.83	5.33 ± 0.75	4.76 ± 0.59	1.66 ± 0.10
Hippocampus	2.07 ± 0.45	2.23 ± 0.16	1.49 ± 0.13	0.98 ± 0.09
Cortex	1.42 ± 0.19	1.57 ± 0.16	1.30 ± 0.15	0.93 ± 0.07
Hypothalamus	3.59 ± 0.42	3.81 ± 0.35	2.51 ± 0.35	1.13 ± 0.07
Remainder	1.87 ± 0.23	2.09 ± 0.22	1.59 ± 0.06	1.03 ± 0.07
Ratio (vs. CB)				
Striatum	4.53 ± 0.91	4.10 ± 0.45	3.85 ± 0.55	1.77 ± 0.22
Hippocampus	1.78 ± 0.29	1.72 ± 0.07	1.20 ± 0.04	1.03 ± 0.08
Cortex	1.23 ± 0.11	1.21 ± 0.05	1.05 ± 0.07	0.99 ± 0.09
Hypothalamus	3.09 ± 0.23	2.94 ± 0.14	2.02 ± 0.20	1.19 ± 0.05
Remainder	1.62 ± 0.07	1.61 ± 0.08	1.29 ± 0.08	1.09 ± 0.05

[a] The concentrations of the impurities added for the 0×, 10×, 100× and 1000× groups were listed proportionally: 0 mg/kg, 0.071 mg/kg (compound **3**, 8.6×10^{-4} mg/kg, compound **6**, 6.1×10^{-2} mg/kg and compound **8**, 8.6×10^{-3} mg/kg), 0.71 mg/kg and 7.1 mg/kg, respectively.

most abundant. The low levels of impurities of the purified product will likely show no effect on the in vivo binding to VMAT2 target binding sites in humans.

3.5. Ex vivo and in vitro autoradiography

Ex vivo and in vitro autoradiography both showed that there were no differences between SPE- and HPLC-purified D6-[^{18}F]FP-(+)-DTBZ, [^{18}F]**9**, and the intensity of binding in the striatum matched well with the known VMAT2 distribution in the brain (Fig. 5). The resulting images corroborated the regional brain tissue dissection data and showed high tracer uptake and retention in regions of brain with higher VMAT2 densities. The competitive binding studies in autoradiography showed that **3** at 5.7 nmol/mL will block [^{18}F]**9** binding. However, **6** and **8** (at 2.7 nmol/mL and 6.0 nmol/mL, respectively) will not block VMAT2 binding, most likely due to their lower binding affinities.

It is important to note that the major difference between HPLC- and SPE-purified D6-[^{18}F]FP-(+)-DTBZ, [^{18}F]**9**, is the amount of residual chemical impurities in the dose. HPLC purification will remove all of the chemical impurities, including compounds **3**, **6** and **8**, while the SPE will only remove the majority of these chemicals, and residual chemical impurities remained (<50 μg of total chemical impurity per production batch). It is important to note that the total chemical amount listed in the package insert per dose of Amyvid ([^{18}F]AV-45, florbetapir F18) is <50 μg of total chemical [34]. Amyvid is manufactured via an HPLC purification method and is commercially distributed. The SPE preparation of D6-[^{18}F]FP-(+)-DTBZ, [^{18}F]**9**, as described in this paper, clearly contained <50 μg of total chemical per dose. The contents of chemical impurities after SPE purification were low; therefore, they are unlikely to influence VMAT2 binding in vivo. The results of the in vivo biodistribution study and autoradiography studies in normal mice also suggested that the impurities at their expected low doses did not affect the biodistribution in the brain, and no significant differences in striatal localization were observed. These results support the use of this SPE purification method to prepare D6-[^{18}F]FP-(+)-DTBZ, [^{18}F]**9**. Future implementation of this method for the routine preparation of multiple doses will facilitate the diagnosis of PD based on changes in VMAT2 binding sites in the basal ganglia regions of the brain.

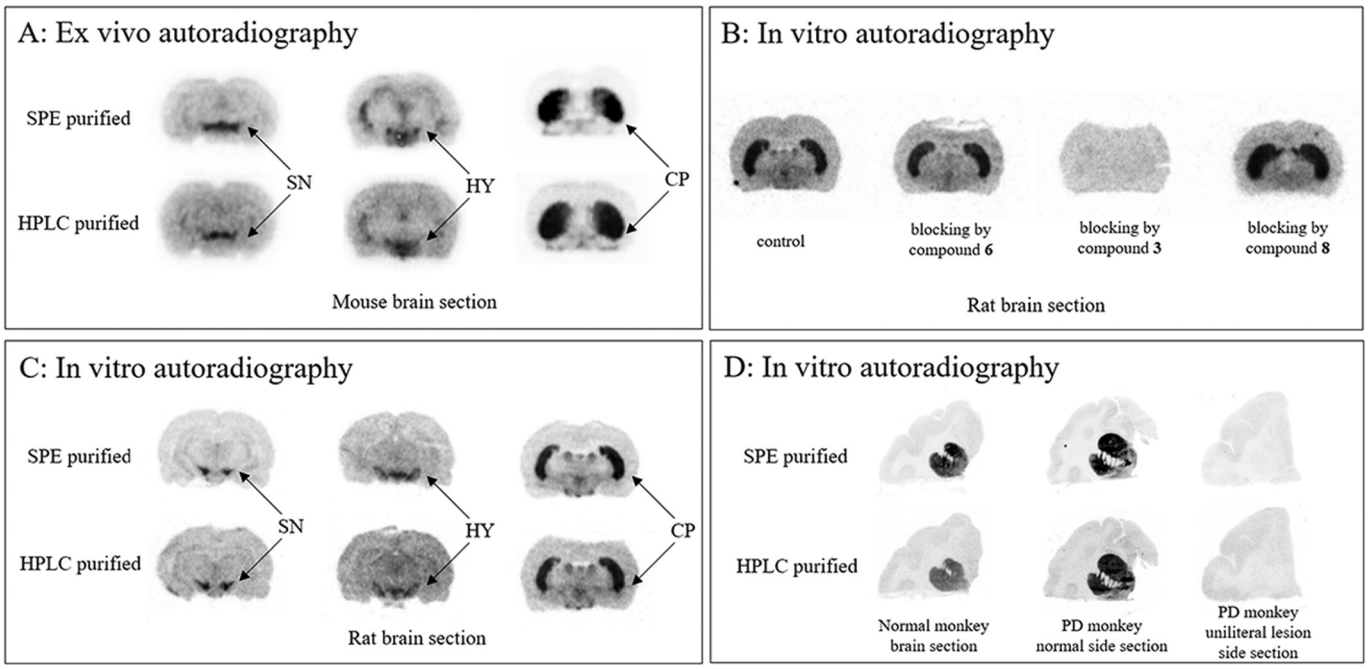

Fig. 5. Autoradiography results. A: Ex vivo autoradiography of mouse brain sections using SPE- and HPLC-purified D6-[^{18}F]FP-(+)-DTBZ, [^{18}F]**9**. Normal CD-1 mice were injected with 19 MBq of SPE- or HPLC-purified [^{18}F]**9**. B: In vitro autoradiography of rat brain sections; VMAT2 binding sites were blocked with **3**, **6** and **8** (the concentrations of competitive compounds **3**, **6** and **8** are 5.7 nmol/mL, 2.7 nmol/mL and 6.0 nmol/mL, respectively). Sections were incubated at room temperature for 30 min with 4.5 MBq of D6-[^{18}F]FP-(+)-DTBZ, [^{18}F]**9**, in 20 mL of buffer solution. C and D: In vitro autoradiography of rat and monkey brain sections using SPE- or HPLC-purified D6-[^{18}F]FP-(+)-DTBZ, [^{18}F]**9**. Same procedure with B. HY: Hypothalamic nucleus, SN: substantia nigra.

4. Conclusion

An improved preparation of D6-[^{18}F]FP-(+)-DTBZ, [^{18}F]**9**, using optimal reaction conditions and solid-phase extraction (SPE) was demonstrated. The desired product was prepared in 35 min in 38.9% RCY (decay corrected) and a high RCP (>99%). This SPE purification method is well suited to automatic synthesis for routine clinical applications. This new VMAT2 imaging agent, D6-[^{18}F]FP-(+)-DTBZ, [^{18}F]**9**, in conjunction with PET imaging, might provide a routine clinical tool for improving the diagnosis of Parkinson's disease (PD).

Abbreviations

AFB	ammonium formate buffer
DTBZ	dihydrotetrabenazine
FDG	2-fluoro-2-dexoy-D-glucose
FES	16α-fluoroestradiol-17β-sulfamate
FMZ	ethyl 8-fluoro-5,6-dihydro-5-methyl-6-oxo-4H-imidazo[1,5-a][1,4]benzodiazepine-3-carboxylate
FP-(+)-DTBZ	9-fluoropropyl-(+)-dihydrotetrabenazine
HED	human equivalent dose
HEPES	4-(2-hydroxyethyl)-1-piperazineethanesulfonic acid
HPLC	high-performance liquid chromatography
HRMS	high-resolution mass spectrometry
LC/MS	liquid chromatography/mass spectrometry
PD	Parkinson's disease
PET	positron emission tomography
RCP	radiochemical purity
RCY	radiochemical yield
SPE	solid-phase extraction
TBZ	tetrabenazine
VMAT2	vesicular monoamine transporter 2

Acknowledgments

This work was supported in part by Five Eleven Pharma Inc. and the Key Field Research and Development Program of Guangdong Province (2018B030337001).

Appendix A. Supplementary data

Supplementary data to this article can be found online at https://doi.org/10.1016/j.nucmedbio.2019.07.002.

References

[1] Kilbourn MR. In vivo radiotracers for vesicular neurotransmitter transporters. Nucl Med Biol 1997;24:615–9.
[2] Albin R, Koeppe R. Rapid loss of striatal VMAT2 binding associated with onset of Lewy body dementia. Mov Disord 2006;21:287–8.
[3] Hayden MR, Leavitt BR, Yasothan U, Kirkpatrick P. Tetrabenazine. Nat Rev Drug Discov 2009;8:17.
[4] Brossi A, Lidlar H, Walter M, Schnider O. Syntheseversuche in der Emetin-Reihe. 2-Oxo-hydrobenzo[a]chinoline. Helv Chim Acta 1958;41:119–39.
[5] Frey KA, Koeppe RA, Kilbourn MR, Vander Borght TM, Albin RL, Gilman S, et al. Presynaptic monoaminergic vesicles in Parkinson's disease and normal aging. Ann Neurol 1996;40:873–84.
[6] Albin R, Koeppe R, Wernette K, Zhuang W, Nichols T, Kilbourn M, et al. Striatal [11C] dihydrotetrabenazine and [11C]methylphenidate binding in Tourette syndrome. Neurology 2009;72:1390–6.
[7] Avendaño-Estrada A, Ávila-Rodríguez MA. Reference tissue models in the assessment of 11C-DTBZ binding to the VMAT2 in rat striatum: a test-retest reproducibility study. Synapse 2018;72:e22029.
[8] Goswami R, Ponde D, Kung M, Hou C, Kilbourn M, Kung H. Fluoroalkyl derivatives of dihydrotetrabenazine as positron emission tomography imaging agents targeting vesicular monoamine transporters. Nucl Med Biol 2006;33:685–94.
[9] Kilbourn M, Hockley B, Lee L, Hou C, Goswami R, Ponde D, et al. Pharmacokinetics of [(18)F]fluoroalkyl derivatives of dihydrotetrabenazine in rat and monkey brain. Nucl Med Biol 2007;34:233–7.
[10] Kung M, Hou C, Goswami R, Ponde D, Kilbourn M, Kung H. Characterization of optically resolved 9-fluoropropyl-dihydrotetrabenazine as a potential PET imaging agent targeting vesicular monoamine transporters. Nucl Med Biol 2007;34:239–46.
[11] Okamura N, Villemagne V, Drago J, Pejoska S, Dhamija R, Mulligan R, et al. In vivo measurement of vesicular monoamine transporter type 2 density in Parkinson disease with 18F-AV-133. J Nucl Med 2010;51:223–8.
[12] Villemagne VL, Okamura N, Pejoska S, Drago J, Mulligan RS, Chetelat G, et al. In vivo assessment of vesicular monoamine transporter type 2 in dementia with lewy bodies and Alzheimer disease. Arch Neurol 2011;68:905–12.
[13] Alexander PK, Lie Y, Jones G, Sivaratnam C, Bozinovski S, Mulligan RS, et al. Management impact of imaging brain vesicular monoamine transporter type-2 (VMAT2) in clinically uncertain Parkinsonian syndrome (CUPS) with 18F-AV133 and PET. J Nucl Med 2017;58:1815–20.
[14] Stoessl AJ, Martin WW, McKeown MJ, Sossi V. Advances in imaging in Parkinson's disease. Lancet Neurol 2011;10:987–1001.
[15] de la Fuente-Fernandez R, Schulzer M, Kuramoto L, Cragg J, Ramachandiran N, Au WL, et al. Age-specific progression of nigrostriatal dysfunction in Parkinson's disease. Ann Neurol 2011;69:803–10.
[16] Strafella AP, Bohnen NI, Perlmutter JS, Eidelberg D, Pavese N, Van Eimeren T, et al. Molecular imaging to track Parkinson's disease and atypical parkinsonisms: new imaging frontiers. Mov Disord 2017;32:181–92.
[17] Hsiao IT, Weng YH, Hsieh CJ, Lin WY, Wey SP, Kung MP, et al. Correlation of Parkinson disease severity and 18F-DTBZ positron emission tomography. JAMA Neurol 2014;71:758–66.
[18] Siderowf A, Pontecorvo MJ, Shill HA, Mintun MA, Arora A, Joshi AD, et al. PET imaging of amyloid with Florbetapir F 18 and PET imaging of dopamine degeneration with 18F-AV-133 (florbenazine) in patients with Alzheimer's disease and Lewy body disorders. BMC Neurol 2014;14:79.
[19] Liu F, Choi SR, Zha Z, Ploessl K, Zhu L, Kung HF. Deuterated (18)F-9-O-hexadeutero-3-fluoropropoxyl-(+)-dihydrotetrabenazine (D6-FP-(+)-DTBZ): a vesicular monoamine transporter 2 (VMAT2) imaging agent. Nucl Med Biol 2018;57:42–9.
[20] Meanwell NA. Synopsis of some recent tactical application of bioisosteres in drug design. J Med Chem 2011;54:2529–91.
[21] Gant TG. Using deuterium in drug discovery: leaving the label in the drug. J Med Chem 2014;57:3595–611.
[22] Kuchar M, Mamat C. Methods to increase the metabolic stability of (18)F-radiotracers. Molecules 2015;20:16186–220.
[23] Pirali T, Serafini M, Cargnin S, Genazzani AA. Applications of deuterium in medicinal chemistry. J Med Chem 2019;62(11):5276–97.
[24] Frank S, Testa CM, Stamler D, Kayson E, Davis C, Edmondson MC, et al. Effect of deutetrabenazine on chorea among patients with Huntington disease: a randomized clinical trial. JAMA 2016;316:40–50.
[25] Ido T, Wan CN, Fowler JS, Wolf AP. Fluorination with F2: a convenient synthesis of 2-deoxy-2-fluoro-D-glucose. J Org Chem 1977;42:2341.
[26] Kuge Y, Nishijima K, Nagatsu K, Seki K, Ohkura K, Tanaka A, et al. Chemical impurities in [18F]FDG preparations produced by solid-phase 18F-fluorination. Nucl Med Biol 2002;29:275–9.
[27] Nakao R, Ito T, Yamaguchi M, Suzuki K. Simultaneous analysis of FDG, ClDG and Kryptofix 2.2.2 in [18F]FDG preparation by high-performance liquid chromatography with UV detection. Nucl Med Biol 2008;35:239–44.
[28] Vaulina D, Nasirzadeh M, Gomzina N. Automated radiosynthesis and purification of [(18)F]flumazenil with solid phase extraction. Appl Radiat Isot 2018;135:110–4.
[29] Fedorova O, Nikolaeva V, Krasikova R. Automated SPE-based synthesis of 16α-[18F] fluoroestradiol without HPLC purification step. Appl Radiat Isot 2018;141:57–63.
[30] Trembath L, Newell M, Devous MD. Technical considerations in brain amyloid PET imaging with 18F-florbetapir. J Nucl Med Technol 2015;43:175–84.
[31] Zhu L, Liu Y, Plossl K, Lieberman B, Liu J, Kung H. An improved radiosynthesis of [(18)F]AV-133: a PET imaging agent for vesicular monoamine transporter 2. Nucl Med Biol 2010;37:133–41.
[32] Zhu L, Qiao H, Lieberman BP, Wu J, Liu Y, Pan Z, et al. Imaging of VMAT2 binding sites in the brain by (18)F-AV-133: the effect of a pseudo-carrier. Nucl Med Biol 2012;39:897–904.
[33] Food and Administration D. Guidance for industry: estimating the maximum safe starting dose in initial clinical trials for therapeutics in adult healthy volunteers. Center for Drug Evaluation and Research (CDER); 2005; 7.
[34] FDA. Amyvid (Florbetapir F18 injection); 2012.